Significant changes to ENSO strength and impacts in the twenty-first century: Results from CMIP5

S. L. Stevenson[1]

Received 14 June 2012; revised 31 July 2012; accepted 1 August 2012; published 12 September 2012.

[1] Changes to the El Niño/Southern Oscillation (ENSO) and its atmospheric teleconnections under climate change are investigated using simulations conducted for the Coupled Model Intercomparison Project (CMIP5). The overall response to CO_2 increases is determined using 27 models, and the ENSO amplitude change based on the multi-model mean is indistinguishable from zero. However, changes between ensembles run with a given model are sometimes significant: for four of the eleven models having ensemble sizes larger than three, the 21st century change to ENSO amplitude is statistically significant. In these four models, changes to SST and wind stress do not differ substantially from those in the models with no ENSO response, indicating that mean changes are not predictive of the ENSO sensitivity to climate change. Also, ocean vertical stratification is less (more) sensitive to CO_2 in models where ENSO strengthens (weakens), likely due to a regulation of the subsurface temperature structure by ENSO-related poleward heat transport. Atmospheric teleconnections also show differences between models where ENSO amplitude does and does not respond to climate change; in the former case El Niño/La Niña-related sea level pressure anomalies strengthen with CO_2, and in the latter they weaken and shift polewards and eastwards. These results illustrate the need for large ensembles to isolate significant ENSO climate change responses, and for future work on diagnosing the dynamical causes of inter-model teleconnection differences. **Citation:** Stevenson, S. L. (2012), Significant changes to ENSO strength and impacts in the twenty-first century: Results from CMIP5, *Geophys. Res. Lett.*, *39*, L17703, doi:10.1029/2012GL052759.

1. Introduction

[2] The El Niño/Southern Oscillation (ENSO) is the dominant source of interannual variability in the Pacific, with substantial socioeconomic impacts both in the tropics and extratropics [*Hoerling et al.*, 1997; *Cai et al.*, 2011]. Thus, understanding the effect of anthropogenic climate change on the nature and severity of ENSO is of great importance. However, there is little agreement in the literature regarding the range of potential ENSO responses to global warming. In the projections performed for phase 3 of the Coupled Model Intercomparison Project (CMIP3), general circulation models (GCMs) were split between ENSO enhancement and damping in the 21st century, independent of overall model performance [*Collins et al.*, 2010]. The causes of these discrepancies are currently not well understood.

[3] Although ENSO amplitude shifts are poorly constrained, future changes to ENSO-relevant atmosphere/ocean physics are fairly robust across models. The mean equatorial ocean stratification is expected to increase [*Timmermann et al.*, 1999], the warm pool to expand eastward and the meridional temperature gradient to increase [*Liu et al.*, 2005], and the equatorial trade winds to weaken [*Vecchi and Soden*, 2007]. An increase in vertical stratification will increase SST sensitivity to thermocline variations, thus enhancing ENSO amplitude. Expansion of the warm pool to the east is thought to favor El Niño triggering by westerly wind bursts [*Eisenman et al.*, 2005], and increasing the meridional temperature gradient to increase ENSO amplitude by making the coupled system less stable [*Sun*, 2003]. However, the net effect of these changes is unknown, and will additionally be sensitive to shifts in surface atmosphere/ocean feedback processes which can favor either ENSO amplification or damping [*Philip and van Oldenborgh*, 2006].

[4] The 'null hypothesis' for the ENSO climate change response, which is often difficult to reject, is natural variability. Long equilibrated GCM simulations [*Wittenberg*, 2009; *Stevenson et al.*, 2012a] show unforced centennial variations in ENSO amplitude of 100% or more. This internal variability requires that at least 250 years of data be averaged together to provide robust ENSO statistics [*Stevenson et al.*, 2010]; since multiple long simulations at varying CO_2 with a stable mean climate are rare, it is difficult to know the true range of model ENSO climate sensitivity [*Stevenson et al.*, 2012b]. The present study seeks to assess the significance of projected 21st century ENSO changes in the CMIP5 archive, and to examine the differences between mean conditions and atmospheric impacts among models with and without a significant response of ENSO to climate change.

2. ENSO Amplitude Response

[5] Previous multi-model ENSO comparisons [*AchutaRao and Sperber*, 2006; *Collins et al.*, 2010] typically included as many models as possible, although only a single ensemble member is available for the majority of models. For comparison with earlier work, all CMIP5 data currently available have been analyzed; this set consists of 27 models (Table 1 in Text S1 in the auxiliary material), and is hereafter referred to as the FULL sample.[1] Given the potential importance of natural variability, particular attention is then focused on those models for which three or more realizations of both the 20th century and at least one of the 21st century

[1]International Pacific Research Center, University of Hawaii at Manoa, Honolulu, Hawaii, USA.

Corresponding author: S. L. Stevenson, International Pacific Research Center, University of Hawaii at Manoa, POST 401, Honolulu, HI 96822, USA. (slgs@hawaii.edu)

0094-8276/12/2012GL052759

[1]Auxiliary materials are available in the HTML. doi:10.1029/2012GL052759.

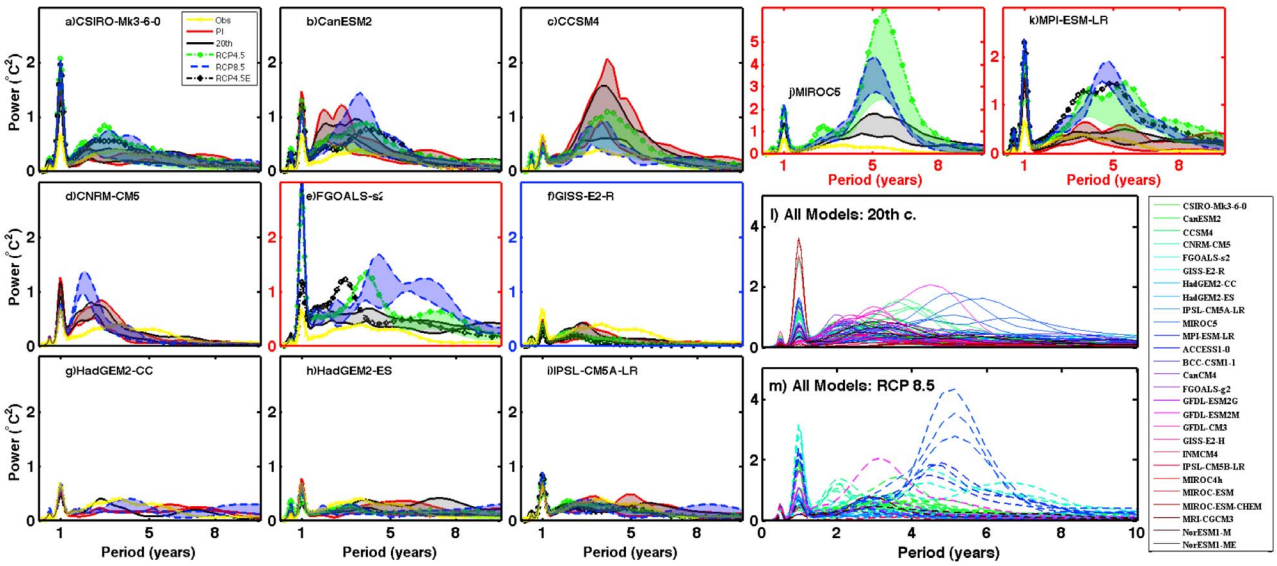

Figure 1. NINO3.4 mean wavelet spectral power, generated using the Morlet wavelet of degree 6 and including only values significant at 90%: shaded regions represent the difference between the maximum and minimum wavelet power in all ensemble members. For the pre-industrial controls, shaded region shows the range for individual centuries of the control run. The yellow line indicates the NINO3.4 SST spectrum from HadSST2 [*Rayner et al.*, 2006]. (a–k) MULTI models. (l) FULL, 20th century. (m) FULL, RCP 8.5 (see Table 1 in Text S1 for full model list). Panels with colored borders have ENSO amplitudes which respond significantly to climate change; red indicates strengthening with CO_2, and blue indicates weakening.

Representative Concentration Pathways (RCPs) have been simulated. The total number of models meeting this criterion is eleven; hereafter these models are referred to as the MULTI sample.

[6] The NINO3.4 SST (5°S–5°N, 190–240°E) wavelet power spectrum is adopted as a metric for ENSO amplitude, and is shown in Figures 1a–1k for each of the models in MULTI. (Note that the results are insensitive to the choice of index region, as seen in Figure 2 in Text S1.) Results for all 27 models are also shown in Figures 1l and 1m. The models show a wide range of ENSO variability: for example, HadGEM2-ES, IPSL CM5A-LR and GISS-E2-R have low spectral power, while ENSO is generally much stronger in the CCSM4, CNRM-CM5 and CanESM2. On the whole, inter-model scatter leads to substantial overlap between 20th century (Figure 1l) and 21st century (here RCP8.5; Figure 1m) ENSO amplitude. The multi-model mean response, in other words, is statistically indistinguishable from zero.

[7] Individual model ensembles also show insignificant ENSO climate change responses in the majority of cases, lending credence to the results from FULL. Comparing Figures 1a–1k shows that 7 of 11 MULTI models (hereafter the NORESP models) have substantial overlap between the 20th century and RCP ensembles, which are confirmed by significance testing to be indistinguishable in these cases (see auxiliary material). This is an indication that previously documented inter-model differences [*Collins et al.*, 2010; *Guilyardi et al.*, 2009] arise partly due to random noise: perhaps models disagree on how ENSO will change in the 21st century, in part, because ENSO *does not always change* during the 21st century. This point is illustrated by the scatter between centuries in the pre-industrial control MULTI simulations (red envelopes of Figures 1a–1k), which is comparable to the range within the 20th century and RCP ensembles; naturally occurring centennial ENSO changes are comparable to the climate change signal in all models.

[8] Interestingly, a significant ENSO response does occur in GISS-E2-R, FGOALS-s2, MIROC5 and MPI-ESM-LR (hereafter the 'RESP' models); in GISS-E2-R ENSO weakens with CO_2, and in the latter three models it strengthens. These models do not systematically differ in ensemble size from NORESP (Figure 1 in Text S1), nor do they differ in the strength of the NINO3.4 SST seasonal cycle (Figure 3 in Text S1). This implies that differences are likely due either to changes to the mean state, or to a shift in the balance among competing feedbacks. A thorough investigation of feedback processes was not possible here; however, mean state metrics are presented in Figure 2 for RCP4.5 (results are insensitive to the choice of RCP ensemble; not pictured). Ensemble-mean equatorial SST warming (Figure 2a, colors) is enhanced in the eastern Pacific, consistent with *Collins et al.* [2010]. The pattern of wind stress changes (Figure 2b, arrows) is likewise consistent with the CMIP3 results of *Xie et al.* [2010]; equatorial warming drives a southerly cross-equatorial flow in the eastern Pacific, which leads to convergence near 5–10°N and divergence near 5–10°S (Figure 2). Along the equator the trades weaken, as required by the reduction in zonal SST gradient and associated Bjerknes feedback. However, no systematic differences between the mean equatorial SST or wind responses to the RESP and NORESP samples are observed (Figures 2c–2f, vertical solid lines). Changes to the zonal and meridional SST gradients in RESP and NORESP are also indistinguishable, and therefore cannot explain the differing ENSO sensitivities to climate change.

[9] The final mean-state metric considered here is the vertical structure of equatorial temperature. The difference between SST and thermocline temperature has been shown [*Sun*, 2003] to affect ENSO amplitude by changing the stability of the system. Here, changes to stratification in the

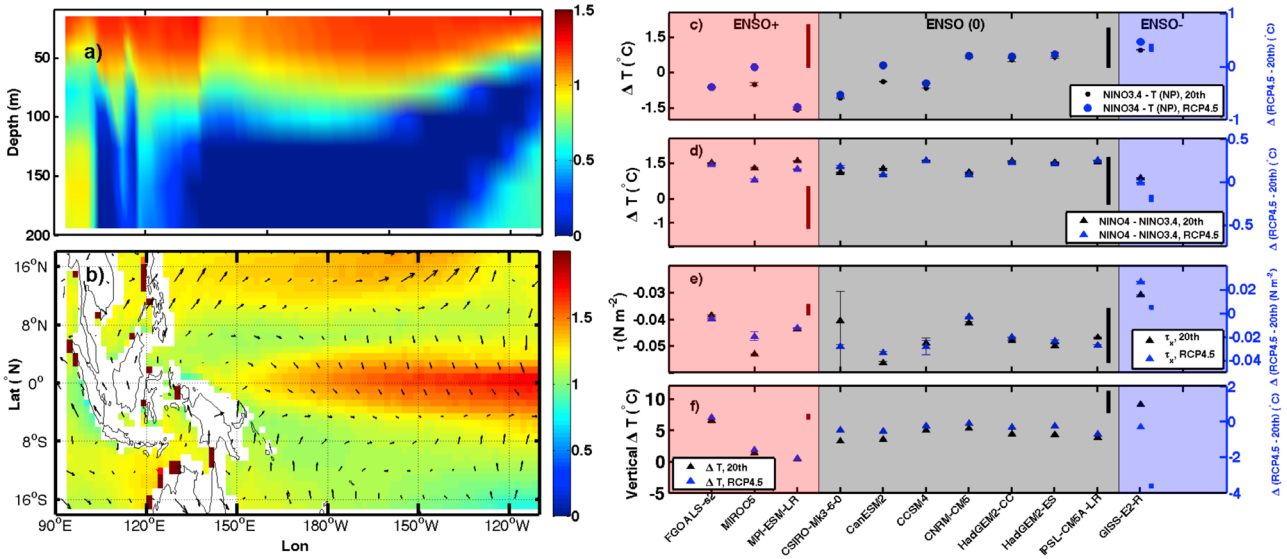

Figure 2. Mean state changes in MULTI (RCP 4.5 - 20th c.). (a) Composite of ensemble-mean temperature changes, averaged over 10–20°N. (b) Changes in SST (colors) and wind stress (vectors). (c) Difference between SST in NINO3.4 and the 'NP' region 10–20°N, 120–170°E. (d) Zonal SST gradient (NINO4 -NINO3.4 SST). (e) Changes to NINO3.4 zonal wind stress. (f) Difference in temperature over 120–170°E, 0–50 m and 120–170°E, 100–150 m. For Figures 2c–2e, the 20th century appears in black and the RCP 4.5 in blue; error bars show the spread between all ensemble members considered. For Figure 2f, vertical temperature profiles used only 1 ensemble member and errors are accordingly omitted. Vertical solid lines in Figures 2c–2f show the range of ensemble-mean RCP4.5 - 20th century differences for all models in each category (ENSO+: ENSO strengthens with CO_2. ENSO(0): no change. ENSO-: ENSO weakens with CO_2).

warm pool (120–180°E, 5°S–5°N) are approximated in Figure 2f as the difference between the temperature averaged over 0–50 m and 100–140 m; most models show temperature differences of 2–4°C in the 20th century, increasing to 4–6°C in RCP4.5. Mean 20th century stratification is similar between models where ENSO does and does not respond to climate change. However, the *changes* to those temperature differences between the 20th century and RCP4.5 are much larger in models where ENSO either weakens or remains constant; of particular note is the GISS-E2-R, where the ENSO amplitude and stratification actually decreases with CO_2.

[10] The results of Figure 2f are precisely what is expected from a 'heat pump'-like ENSO [*Sun and Zhang*, 2006], where ENSO variability acts to equalize an imposed heating anomaly, resulting in a negative feedback on stratification changes (see Figure 4 in Text S1 for the composite subsurface temperature structure responses). Variations in the strength of the ENSO 'heat pump' would also explain the fact that trends in the difference of total ocean heat content between 5°S–5°N and 10–20°N are relatively small (Figure 5 in Text S1); ENSO is a plausible mechanism for maintaining the balance between equatorial and off-equatorial heat content in the presence of transient climate change. However, it is important to note that the present analysis constitutes only circumstantial evidence, as simulations with prescribed heat content anomalies could not be performed with each model; further analysis will be required to confirm these results.

3. Atmospheric Teleconnections

[11] The present teleconnection analysis follows *Stevenson et al.* [2012b], where compositing is used to determine the changes to surface air temperature (SAT) and sea level pressure (SLP) anomalies associated with El Niño and La Niña; particular attention is paid to the Aleutian Islands, Australia and the high-latitude Southern Ocean, to follow on from previous studies [*Meehl and Teng*, 2007; *Cai et al.*, 2011]. Teleconnection changes are then evaluated by comparing the RCP4.5 and 20th century ensembles, and all values have been normalized to the total ensemble-member ENSO variance prior to averaging. In RCP4.5 relative to the 20th century (Figure 3a, contours), El Niño teleconnections tend to weaken, possibly resulting partly from changes to the static stability of the atmosphere [*Ma et al.*, 2012]. In addition, both the Aleutian and Southern Ocean teleconnections also shift poleward and eastward with CO_2; this was observed in CMIP3 by *Meehl and Teng* [2007] and *Kug et al.* [2010] and in CCSM4 by *Stevenson et al.* [2012b].

[12] Twentieth century La Niña teleconnections (Figure 3b) are primarily an inverse of the El Niño patterns, with some possible minor asymmetries (e.g., anomalies over the Southern Ocean). The Aleutian La Niña teleconnection strengthens overall and expands longitudinally in RCP4.5, with little overall change in position. This small shift in the Aleutian SLP anomaly contrasts with previous results using CMIP3 models, which showed eastward shifts in both El Niño and La Niña SLP teleconnections due to a change in the position of tropical convective anomalies [*Kug et al.*, 2010]. The diversity of models in Figure 3b likely accounts for some of the differences, as no attempt has been made to exclude models based on performance (see Figures 6–15 in Text S1 for individual model teleconnections).

[13] The results from the MULTI models are shown in Figures 3e and 3f, and show substantial differences in the teleconnection response between models in which ENSO does and does not strengthen with CO_2. MPI-ESM-LR, MIROC5 and FGOALS-s2 show a tendency for both El Niño and La Niña teleconnections to strengthen 'in place'

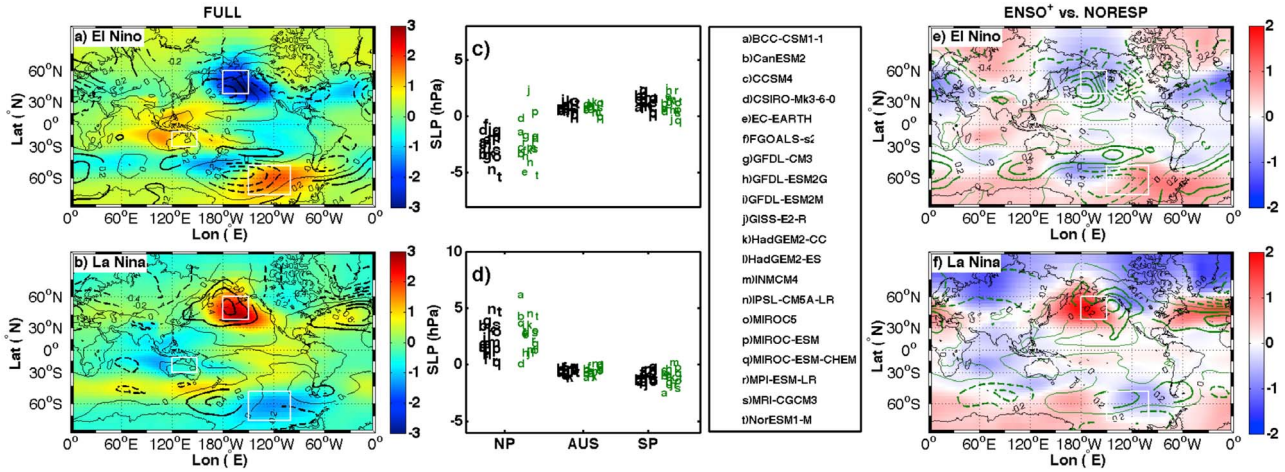

Figure 3. DJF ENSO teleconnections. (a and b) 20th century mean SLP anomaly (colors) and difference between RCP 4.5 and the 20th century (contours). Dashed contours indicate negative SLP anomalies. a) El Niño and b) La Niña events: DJF surface temperature anomaly exceeded +/−1 σ relative to a linearly detrended mean state. (c and d) The mean values for the 20th century and RCP4.5, calculated in the boxed regions from Figures 3a and 3b. 'NP', 'AUS' and 'SO' refer to the North Pacific (Aleutian Low), Australasia, and the Southern Ocean respectively. Individual models are indicated by the letters drawn in Figures 3c and 3d: 20th century anomalies are shown in black, and RCP 4.5 anomalies in green. Figures 3e and 3f show the RCP4.5 - 20th century difference in DJF SLP, for the 'ENSO+' models MPI-ESM-LR, MIROC5 and FGOALS-s2 (colors) and for the 'NORESP' models (contours). Conventions for Figures 3 and 3f are identical otherwise to Figures 3a and 3b.

(Figures 3e and 3f, colors), while the NORESP models more faithfully reproduce the pattern seen in FULL and in *Meehl and Teng* [2007] and *Kug et al.* [2010] (Figures 3e and 3f, contours) including the eastward shift of the North and South Pacific teleconnections for both El Niño and La Niña. Thus, the magnitude of the ENSO amplitude response to climate change is crucial for understanding both the changes in position and intensity of circulation anomalies.

[14] Finally, the degree of variability in teleconnection strength for the three regions of interest is shown in Figures 3c and 3d. There is a large amount of variation in the SLP anomalies in all three regions; the North Pacific seems to be most variable, as SLP anomalies averaged over this region are quite sensitive to the position of the Aleutian Low. Scatter for Australasia and the Southern Ocean is on the order of 0.5 hPa, which is substantial in comparison with the anomalies themselves and highlights the importance of diagnosing the causes for inter-model differences. A complete analysis is beyond the scope of this study; however, the scatter in the regional averages of Figure 3c clearly demonstrates that differences in model physics do lead to detectable changes not only in the ENSO teleconnections themselves, but in the teleconnections' sensitivity to climate change.

4. Discussion and Conclusions

[15] The response of ENSO variability to climate change is examined in 27 CMIP5 models, and the multi-model mean for the RCP projections shows ENSO amplitudes indistinguishable from the 20th century. Additionally, in seven of the eleven models which have at least three ensemble members in at least two ensembles, the 21st and 20th century ENSO amplitudes are statistically identical. The ENSO response to CO_2 increases in the remaining four models does not result from changes to ensemble size, the SST seasonal cycle, or mean SST and wind stress; ENSO climate sensitivities are likely a function of changes to atmosphere/ocean feedbacks [*Philip and van Oldenborgh*, 2006]. A potential influence of ENSO changes on the subsurface temperature structure is also documented; in all three models (MPI-ESM-LR, MIROC5, FGOALS-s2) where ENSO strengthens with CO_2, the temperature difference across the main thermocline is much less sensitive to climate change, consistent with the 'heat pump' of *Sun and Zhang* [2006].

[16] The ensemble-mean El Niño teleconnection response is consistent with CMIP3 results [*Meehl and Teng*, 2007; *Kug et al.*, 2010]: the North Pacific teleconnection shifts northeastward and the overall strength of SLP teleconnections weakens. Changes to La Niña teleconnections show a strengthening of the high pressure system over the Aleutians, and a smaller mean eastward shift; other teleconnections are closer to the inverse of the El Niño pattern. In models where ENSO amplitude increases with CO_2, teleconnections tend to strengthen, and do not shift position. This likely relates to the changing importance of shifts in the intensity *versus* location of tropical convective heating anomalies, and highlights the relevance of ENSO amplitude changes for teleconnection studies. Finally, large inter-model differences are documented in all regions examined; this is recommended for future investigation.

[17] **Acknowledgments.** The author thanks B. Fox-Kemper, E. Guilyardi, M. Jochum, G. Meehl, D.-Z. Sun, and S.-P. Xie for discussions and suggestions which have greatly strengthened the paper.

[18] The Editor thanks the two anonymous reviewers for assisting in the evaluation of this paper.

References

AchutaRao, K., and K. R. Sperber (2006), ENSO simulation in coupled ocean–atmosphere models: Are the current models better?, *Clim. Dyn.*, *27*(1), 1–15.

Cai, W., P. van Rensch, T. Cowan, and H. H. Hendon (2011), Teleconnection pathways of ENSO and the IOD and the mechanisms for impacts on Australian rainfall, *J. Clim.*, *24*, 3910–3923.

Collins, M., et al. (2010), The impact of global warming on the tropical Pacific Ocean and El Niño. *Nat. Geosci.*, *3*, 391–397, doi:10.1038/NGEO868.

Eisenman, I., L. Yu, and E. Tziperman (2005), Westerly wind bursts: ENSO's tail rather than the dog?, *J. Clim.*, *18*, 5224–5237.

Guilyardi, E., A. Wittenberg, A. Fedorov, M. Collins, C. Wang, A. Capotondi, G. Jan van Oldenborgh, and T. Stockdale (2009), Understanding El Niño in ocean-atmosphere general circulation models: Progress and challenges, *Bull. Am. Meteorol. Soc.*, *90*, 325–340.

Hoerling, M., A. Kumar, and M. Zhong (1997), El Niño, La Niña, and the nonlinearity of their teleconnections, *J. Clim.*, *10*, 1769–1786, doi:10.1175/1520-0442(1997)010<1769:ENOLNA>2.0.CO;2.

Kug, J.-S., S.-I. An, Y.-G. Ham, and I.-S. Kang (2010), Changes in El Niño and La Niña teleconnections over North Pacific-America in the global warming simulations, *Theor. Appl. Climatol.*, *100*, 275–282, doi:10.1007/s00704-009-0183-0.

Liu, Z., S. Vavrus, F. He, N. Wen, and Y. Zhong (2005), Rethinking tropical ocean response to global warming: The enhanced equatorial warming, *J. Clim.*, *18*, 4684–4700.

Ma, J., S. Xie, and Y. Kosaka (2012), Mechanisms for tropical tropospheric circulation change in response to global warming, *J. Clim.*, *25*, 2979–2994.

Meehl, G. A. and H. Teng (2007), Multi-model changes in El Niño teleconnections over North America in a future warmer climate, *Clim. Dyn.*, *29*, 779–790, doi:10.1007/s00382-007-0268-3.

Philip, S., and G. J. van Oldenborgh (2006), Shifts in ENSO coupling processes under global warming, *Geophys. Res. Lett.*, *33*, L11704, doi:10.1029/2006GL026196.

Rayner, N., P. Brohan, D. E. Parker, C. F. Folland, J. J. Kennedy, M. Vanicek, T. Ansell, and S. Tett (2006), Improved analyses of changes and uncertainties in sea surface temperature measured in situ since the mid-nineteenth century: The HadSST2 data set, *J. Clim.*, *19*(3), 446–469.

Stevenson, S., B. Fox-Kemper, and M. Jochum (2012a), Understanding the ENSO-CO_2 link using stabilized climate simulations, *J. Clim.*, doi:10.1175/JCLI-D-11-00546.1, in press.

Stevenson, S., B. Fox-Kemper, M. Jochum, R. Neale, C. Deser, and G. Meehl (2012b), Will there be a significant change to El Niño in the 21st century? *J. Clim.*, *25*, 2129–2145, doi:10.1175/JCLI-D-11-00252.1.

Stevenson, S., B. Fox-Kemper, M. Jochum, B. Rajagopalan, and S. Yeager (2010), Model ENSO validation using wavelet probability analysis, *J. Clim.*, *23*, 5540–5547.

Sun, D.-Z. (2003), A possible effect of an increase in the warm-pool sst on the magnitude of El Niño warming, *J. Clim.*, *16*(2), 185–205.

Sun, D.-Z., and T. Zhang (2006), A regulatory effect of ENSO on the time-mean thermal stratification of the equatorial upper ocean, *Geophys. Res. Lett.*, *33*, L07710, doi:10.1029/2005GL025296.

Timmermann, A., J. Oberhuber, A. Bacher, M. Esch, M. Latif, and E. Roeckner (1999), Increased El Niño frequency in a climate model forced by future greenhouse warming, *Nature*, *398*, 694–697.

Vecchi, G., and B. Soden (2007), Global warming and the weakening of the tropical circulation, *J. Clim.*, *20*, 4316–4340, doi:10.1175/JCLI4258.1.

Wittenberg, A. T. (2009), Are historical records sufficient to constrain ENSO simulations?, *Geophys. Res. Lett.*, *36*, L12702, doi:10.1029/2009GL038710.

Xie, S.-P., C. Deser, G. Vecchi, J. Ma, H. Teng, and A. Wittenberg (2010), Global warming pattern formation: Sea surface temperature and rainfall, *J. Clim.*, *23*, 966–986.